Non-linear Oscillations Assessment of the Distribution Static Compensator Operating in Voltage Control Mode

J. SEGUNDO-RAMÍREZ,[1] AURELIO MEDINA,[2]
ARINDAM GHOSH,[3] and GERARD LEDWICH[3]

[1]Universidad Autónoma de San Luis Potosí, CIEP-FI, San Luis Potosí, S.L.P., México
[2]Facultad de Ingeniería Eléctrica, División de Estudios de Postgrado, UMSNH, Morelia, Michoacán, México
[3]School of Engineering Systems, Queensland University of Technology, Brisbane, Queensland, Australia

Abstract – This paper deals with the nonlinear oscillations assessment of a DSTATCOM operating in voltage control mode, using bifurcation theory. The mathematical model of the DSTATCOM in voltage control mode to carry-out the bifurcation analysis is derived. The stability regions in the Thevenin equivalent plane are computed. In addition, the stability regions in the control gains space, as well as the contour lines for different Floquet multipliers are computed. The ac capacitor and dc capacitor impact on the stability are analyzed through bifurcation theory. The observations are verified through simulation studies. The computation of the stability region allows the assessment the stable operating zones for a power system that includes a DSTATCOM operating in voltage mode.

Keywords: DSTATCOM, Floquet multiplier, Neimark-Sacker bifurcation, nonlinear oscillations, point common coupling, and stability region.

I. INTRODUCTION

In general, an electric system varies smoothly with small changes in the system parameters. However, under certain circumstances, a small change in the system parameters could result in a significant qualitative change in the system properties. By definition, bifurcations occur at those parameters values (bifurcation points) where there is a change in the characteristic properties of a system, as well as in the number and type of solutions. Bifurcations have severe impact in the system behaviour, even in normal operations, because they delimit different operating zones. For this reason, the study of bifurcations is useful for practical design. The knowledge of the set of bifurcation values in the parameter space allows us to design of an electrical circuit with the optimal operating conditions. Therefore, an important problem in dynamic nonlinear circuits is the investigation of the set of bifurcation values in the parameter space [1]-[2]. In this paper, we analyze the nonlinear oscillations produced in an electric network including a distribution static compensator (DSTATCOM) operating in voltage control mode [3].

The common adopted technique to analyze the stability in an electric network including a DSTATCOM device is the brute force approach or eigen analysis [4]. The brute force method is based on the direct application of a numerical integration method to investigate the trajectories of the state variables. However, this method is limited to the investigation of asymptotically stable steady states. In

the eigenanalysis, the system is linearized around an equilibrium operating point. The stability is of this point is determined by computing the eigenvalues. However, in this conventional stability analysis, the power system is represented in root mean square (RMS) quantities, and the network transients are neglected.

To explore both stable and unstable limit cycles [1], a different technique has to be considered. A suitable framework is the bifurcation analysis; a nonlinear mathematical theory [1]-[2] used to qualitatively investigate how the integral curves change as the parameters are varied. The bifurcation theory has been applied to the analysis of voltage collapse [5], analysis of the Electric Arc Furnace (EAF) [6], chaotic oscillations [7], ferroresonance analysis [8], and the design of nonlinear controllers [9]. It has also been applied to assess the dynamic behaviour of nonlinear components such as induction motors [10], load models [11]-[12], tap changing transformers [13], and flexible ac transmission system (FACTS) devices [14], [15]. However, this theory has not yet been used to assess the loss of stability in a DSTATCOM operating in voltage control mode connected to the electric network.

In power electronics, the bifurcation theory has been used successfully to analyze the stability of power converters and switched circuits [16]-[23]. Conventionally, this analysis is carried-out with the discrete-time iterative mapping approach [17]-[22]. Under this approach, the switching converter is essentially modeled as piecewise switched circuits. This results in a nonlinear time-varying operating mode, which naturally demands the use of nonlinear theory [22]. In the discrete-time iterative mapping approach, it is assumed that the network is linear time-invariant between switching instants. Thus, the solution between switches can be found in a closed-form. The nonlinearity comes from the switching control.

Since the network between switching instants is nonlinear due to the nonlinear load in the network, it is not easy to represent the DSTATCOM mathematical model through a discrete-time iterative mapping approach. For this reason, the continuous model based on the energy preservation principle is proposed to carry-out the stability analysis based on the bifurcation theory using a continuation scheme to trace-up the stability boundaries. The bifurcation analysis based on continuation schemes allows us to identify not only the stability boundaries but the type of dynamics in each region, as well as the type of bifurcation that emerges in the system.

This article is organized as follows: Section 2 describes the DSTATCOM operating in voltage control mode. Additionally, a simplified representation of the DSTATCOM is proposed based on a continuous set of ordinary differential equations (ODEs). Section 3 gives a concise description of the continuation techniques and the bifurcation theory. Section 4 presents the results of the bifurcation analysis, and Section 5 presents a discussion of the results.

II. DSTATCOM OPERATING IN VOLTAGE CONTROL MODE

The basic purpose of the DSTATCOM is to compensate the load currents in such a way that at the point of common coupling (PCC) the source current and the PCC voltage are balanced and sinusoidal. There are various algorithms for load compensation with shunt connected devices, such as the DSTATCOM [3], [24]-[28]. Most of these algorithms assume the source voltages to be balanced and sinusoidal. In practice, however, the loads are remote from the distribution substations and are supplied by feeders. Under this situation, the source is termed as non-stiff or weak. The reference compensator currents generated by these algorithms for load compensation are tracked-down using a voltage source converter (VSC) in a hysteresis modulation technique [3]. As a consequence of this, the compensated source currents contain the inverter switching frequency components. This will result on distorted terminal voltages at the PCC due to the feeder impedance. Now, these distorted PCC voltages are taken as input voltage signals by algorithms for load compensation, which generally assume a

balanced voltage supply. Therefore, the control algorithms generate erroneous reference filter currents and consequently the source currents are also distorted. Thus, it is easy to infer that the direct application of these algorithms for load compensation with a non-stiff source results on distorted PCC voltages and severely distorted source currents. In this paper, the control strategy proposed in [3] is used. With this algorithm, the DSTATCOM operates as a voltage regulator to maintain constant the voltage of a specified bus (PCC). The magnitude of the bus voltage is pre-specified, while its phase angle is generated from a dc capacitor control loop. A deadbeat controller for the inverter is used for voltage tracking. With this algorithm, the DSTATCOM can compensate the terminal voltage, irrespective of any distortion or unbalance in the load or in the voltage source. For more details about this algorithm, please refer to [3].

A. DSTATCOM structure

To cancel-out unbalance or harmonics in the terminal voltage at the PCC bus, the converter that constitutes the DSTATCOM must be able to inject currents in one phase, independently of the other two phases. The DSTATCOM structure used in this analysis consists of three H-bridge voltage source converters connected to a common dc storage capacitor, as shown in Fig. 1. Each VSC is connected to the network through a transformer. The transformers are used to provide isolation between the inverter legs. This also prevents the dc capacitor from short circuits between phases. The DSTATCOM based on this structure can independently compensate each phase. It is to be noted that due to the presence of transformers, this topology is not suitable for canceling any dc component in the load current [29]. The inductance L_f represents the leakage inductance of each transformer and the additional external inductance, if any. The switching losses of an inverter and the copper loss of the connecting transformer are represented by a resistance R_f.

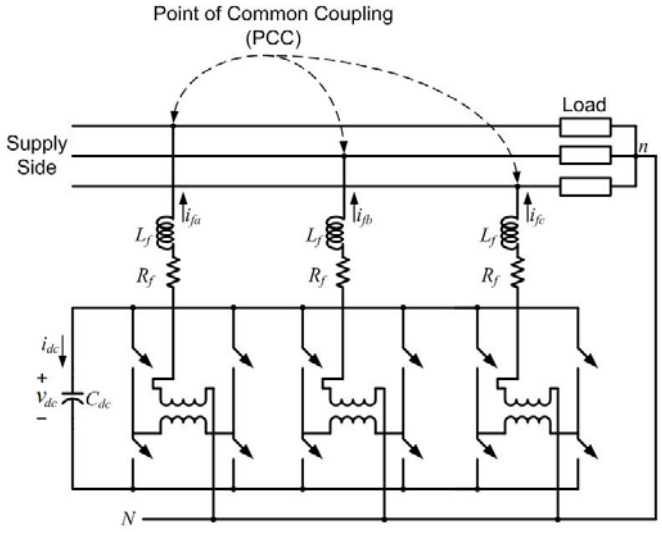

Fig. 1 Structure of the DSTATCOM.

B. DSTATCOM models

In the detailed model, the switches are IGBTs/diodes, the hysteresis modulation scheme, and the dc circuit are explicitly represented. The modeling of the three H-bridge converters and their switching control can be directly done in any EMTP-type simulator. In this contribution, the DSTATCOM detailed

model has been implemented in Power BlockSet/SIMULINK [30].

For our analysis, the detailed model, in which the commutation process is explicitly represented, is not suitable because of the difficulty to compute, to a high precision, the limit cycle and for assessing its stability. For this reason, we propose a simplified model, where the link between the dc side and the ac side is well represented using the energy conservation principle.

In the simplified model, the three H-bridge converters are replaced by three controllable voltage sources. The main advantage of this model is to allow larger integration steps. Besides, the limit cycle can be computed using a shooting method and its stability can be directly assessed. Moreover, this model is suitable for dynamic studies using instantaneous or phasor variables for the network representation, if the harmonic distortion is not taken into account.

In Fig. 2, the schematic representation for the simplified model of DSTATCOM operating in voltage mode is shown. This model is based on the assumption that $v_{tx} = v_{tx}^*$, where v_{tx}^* is the reference terminal voltage. Figure 3 shows the schematic representation of the dc link model.

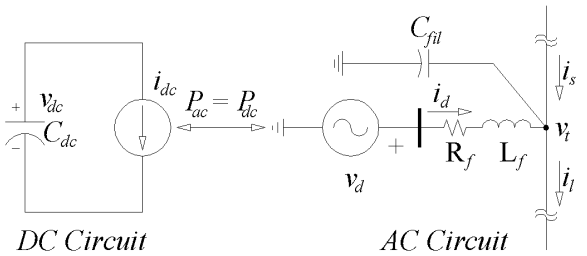

Fig. 2 Schematic representation for the simplified model.

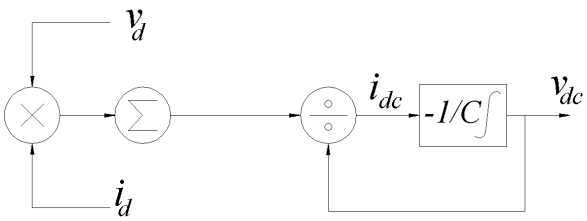

Fig. 3 dc link model.

The reference terminal voltage v_{tx}^* is

$$v_{tx}^* = V_m \sin(\omega t - \delta - \phi_x) \tag{1}$$

and δ is computed using a proportional-integral controller described by,

$$\delta = K_{p\delta}\left(P_{sh} - P_{sh}^*\right) + K_{i\delta}\int\left(P_{sh} - P_{sh}^*\right)\,dt \tag{2}$$

P_{sh} is the instantaneous power reference in the shunt link and P_{sh}^* is its reference; P_{sh} is given by

$$P_{sh} = v_{ta}i_{fa} + v_{tb}i_{fb} + v_{tc}i_{fc} \tag{3}$$

P_{sh}^* is obtained as,

$$P_{sh}^* = K_{pdc}\left(v_{dc}^{average} - v_{dc}^*\right) + K_{idc}\int\left(v_{dc}^{average} - v_{dc}^*\right)\,dt \tag{4}$$

where v^*_{dc} is the reference dc voltage, $v_{dc}^{average}$ is the average voltage across the dc capacitor.

The converter terminal voltage is given by,

$$v_{dx} = R_f i_{dx} + L_f \frac{di_{dx}}{dt} + v_{tx} \tag{5}$$

The current injected by the compensator is calculated by,

$$i_{dx} = -C_{fil} V_m \sin(\omega t - \delta - \phi_x)\left(\omega - \frac{d\delta}{dt}\right) + i_{lx} - i_{sx} \tag{6}$$

The first derivative of i_{dx} is computed as,

$$\frac{di_{dx}}{dt} = \frac{d(i_{lx} - i_{sx})}{dt} - C_{fil} V_m \left(\sin(\omega t - \delta - \varphi_x)\frac{d^2\delta}{dt^2} + \cos(\omega t - \delta - \varphi_x)\left(\omega - \frac{d\delta}{dt}\right)^2\right) \tag{7}$$

The dynamic capacitor voltage is given by,

$$C_{dc}\frac{dv_{dc}}{dt} = -\frac{i_d v_d}{v_{dc}} \tag{8}$$

where

$x = a, b, c$

$\phi_a = 0$

$\phi_b = 2\pi/3$

$\phi_a = -2\pi/3$

$$\frac{d\delta}{dt} = K_{p\delta}\left(\frac{dP_{sh}}{dt} - K_{pv}\frac{dv_{dc}^{average}}{dt}\right) + K_{i\delta}\left(P_{sh} - P_{sh}^{*}\right) \tag{9}$$

$$\frac{d^2\delta}{dt^2} = K_{p\delta}\left(\frac{d^2P_{sh}}{dt^2} - K_{pv}\frac{d^2v_{dc}^{average}}{dt^2}\right) + K_{i\delta}\left(\frac{dP_{sh}}{dt} - K_{pv}\frac{dv_{dc}^{average}}{dt}\right) \tag{10}$$

In comparison to the detailed model, the simplified model is advantageous, since the simplified model can be only described with an ODEs set. In addition, the simplified model can achieve a higher precision than the detailed model and it does not need small integration steps. There are some disadvantages with the simplified DSTATCOM model. Basically, the high frequency phenomena are neglected. However, to avoid erroneous interpretations in our analysis, the bifurcation diagrams are validated against time domain simulations carried-out with the detailed model.

C. Comparative analysis

In this section, the performance of the simplified DSTATCOM model is compared against the detailed model. The system parameters and the DSTATCOM parameters for the circuit shown in Fig. 4 are given in the Appendix A. The hysteresis band for the detailed model is h=10. Please notice that an EAF, a highly nonlinear load is represented in the test case of Fig.4. The dynamic behavior of the $v - i$ characteristic of the EAF is described by a differential equation [32]. This differential equation is based on the principle of energy balance. Starting from the power balance equation for the electric arc, the following differential equation is derived [32]:

$$K_1 r^n + K_2 r\frac{dr}{dt} = \frac{K_3}{r^{m+2}} i_l^2 \tag{4}$$

Here the arc radius r is chosen as state variable. The arc voltage V_{eaf} is given by

$$V_{eaf} = \frac{i_l}{g} \tag{5}$$

where g is the arc conductance and given by the following equation:

$$g = \frac{r^{m+2}}{K_3} \tag{6}$$

It is possible to represent the different stages of the arcing process by simply modifying the parameters of m and n in (1). The complete set of combinations of these parameters for different stages of the electric arc can be found in [32]. The parameters for the EAF used in this investigation are given in Table A1 of Appendix A.

R_l and L_l represent the resistance and the reactance of the flexible cables, the bus conductors, and the graphite electrodes. The dynamic variation of arc resistance and inductance is represented by V_{eaf}, which is given by the equations (4), (5), and (6).

Initially, the electric system is in periodic steady state and the switch sw is open. At t=0 s, the switch sw is closed, thus, the DSTATCOM starts to regulate the terminal voltage v_t at the PCC bus. Figure 5 shows the time domain solution comparison between the detailed and the simplified model, e.g. Fig. 5(a) for the phase angle δ, Fig. 5(b) for the voltage across the dc capacitor v_{dc}, and Fig. 5(c) for the compensation current i_{fa} . The results show a very good agreement between the simplified model and the detailed model, with an integration step size of 60μs and 1μs, respectively. An excellent agreement between the two models is achieved, even though the simplified model uses a considerably larger integration step. The detailed model needs of a small integration step to avoid the numerical error introduced by the commutation process.

The strong correlation between the detailed model and the simplified model results is further illustrated in Fig. 6, which shows the harmonic spectrum for the compensation current i_{fa}. Please observe that the compensation current i_f contains harmonics in order to mitigate the harmonic distortion produced by the nonlinear load.

III. BIFURCATION THEORY AND CONTINUATION METHODS

The set of equations used to represent the electric system can be solved by conventional numerical integration methods to assess the dynamic behaviour of the state variables. However, it is possible with bifurcation theory to predict the behaviour of the solutions without resorting to the numerical integration of the differential equations. The results obtained with the bifurcation analysis can be shown in a bifurcation diagram, which provides qualitative information about the behavior of the steady state solutions. At certain points (bifurcation points) infinitesimal changes in system parameters can cause significant qualitative changes in periodic solutions.

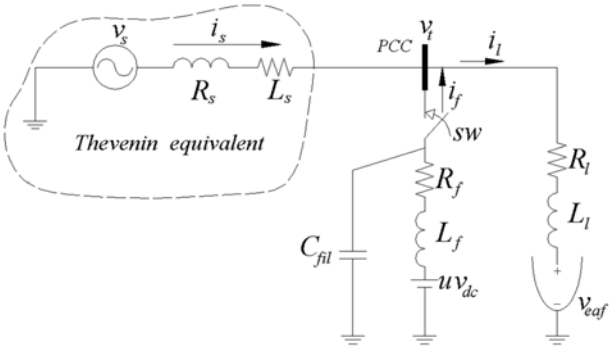

Fig. 4 Compensation of the EAF when the source is non-stiff and the DSTACOM contains a passive filter.

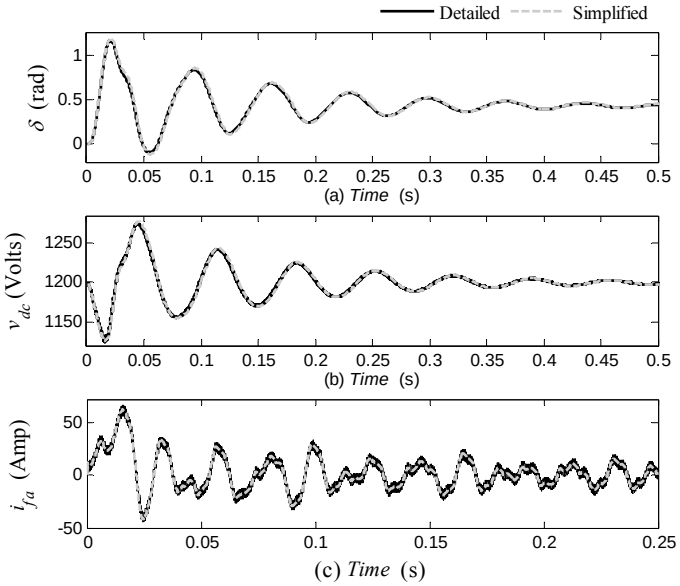

Fig. 5 Comparison in the time domain between the detailed and the simplified model for (a) phase angle δ, (b) dc capacitor voltage v_{dc}, and (c) compensation current i_{fa}.

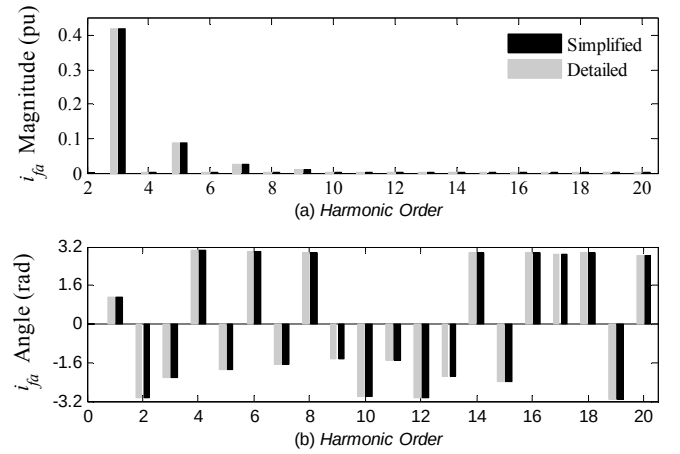

Fig. 6 Spectrum comparison between the detailed and the simplified model for i_{fa}.

A continuation algorithm can trace the path of an already established solution, as the parameters are varied; these parameters are called continuation parameters. In this paper, the sequential method [2] is used as the predictor; in this method, the periodic solution determined in the previous step is used as an initial guess for the periodic solution to be determined in the next step. This method is also known as natural parameter bifurcation [1]. This method fails to go past a turning point in the state-control space [2] since the Jacobian matrix of the associated Poincaré map becomes singular. To avoid this problem, one of the variables x_i is used as a continuation parameter instead of one of the initial continuation parameters. In general, any independent variable or a parameter can be selected as a continuation parameter. After the third point, an extrapolation method based on the cubic spline is used as a predictor. The Newton method based on numerical differentiation (ND) [31] process is used as the corrector. This continuation method is schematically explained in Fig. 7. In this Figure, x_i is a state variable.

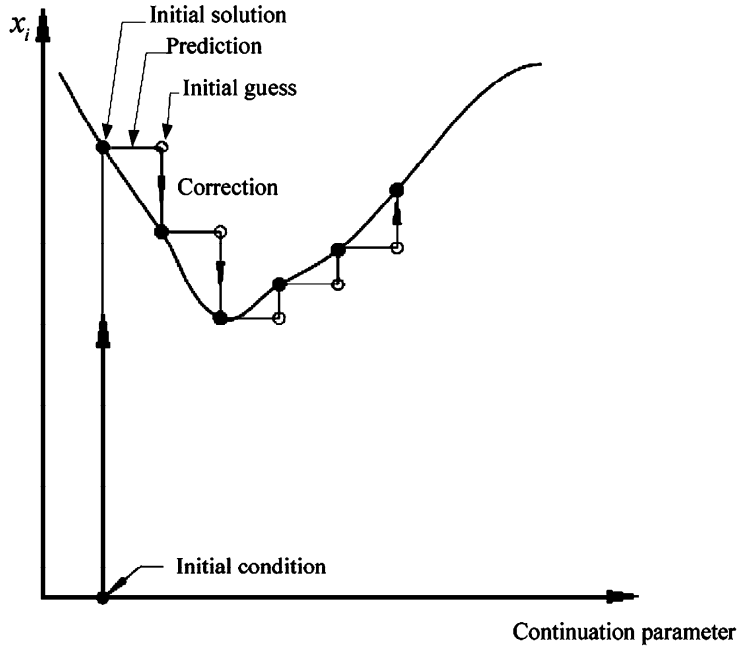

Fig. 7 Sequential continuation method

The stability of a periodic solution is computed from its Floquet multipliers; they describe the stability around the limit cycle of interest. Floquet theory is based on the fact that a periodic solution can be represented through a fixed-point of an associated Poincaré map [1]-[2]. Consequently, the stability of a periodic solution can be determined by computing the stability of the corresponding fixed-point of the Poincaré map. The Floquet multipliers are the eigenvalues of the Jacobian of this Poincaré map. Stable periodic solutions correspond to Floquet multipliers inside the unit circle; on the other hand, unstable periodic solutions have at least one characteristic multiplier outside the unit circle. Therefore, loss of stability is encountered when a multiplier leaves the unit circle. The resulting bifurcation depends on the way the Floquet multipliers leave the unit circle [2]

IV. DSTATCOM STABILITY ANALYSIS BASED ON BIFURCATION THEORY

In this section, the bifurcation theory is applied to the electric system shown in Fig. 4 to assess the stability regions of the electric system including the DSTATCOM operating in voltage control mode. The bifurcations in a power system are basically produced by the nonlinear loads and nonlinear elements. In particular, the DSTATCOM is a nonlinear element due to its controllers and its compensation algorithm.

The loss of stability occurs when at least one Floquet multiplier leaves the unit circle. The nonlinear system can experience several types of bifurcations: for instance, after the first bifurcation, the system can reach a stable operating point in the subsequent bifurcation. However, in this paper, only the first bifurcation is included in the stability regions. The reason to do this is because after the first bifurcation, the electric system losses stability and the protecting devices disconnect the DSTATCOM from the PCC bus.

In the section to follow, bifurcation diagrams in the Thevenin space are computed to show the set of L_s, R_s, and v_s (derived from Thevenin reactance) for which the DSTATCOM contains stable solutions. The stability regions in the gains space are calculated through bifurcation theory, and the set of gains for the fastest speed response of the DSTATCOM is obtained from this analysis. Besides, the gains

impact on the stability regions in the Thevenin space is analyzed. Finally, the ac and dc capacitors impact on the stability in the Thevenin space is analyzed.

The simplified DSTATCOM model is used in this analysis; however, the solutions will be compared against the detailed DSTATCOM model to validate the results. The simplified model is used in this analysis rather than the detailed model basically because the detailed model does not allow the correct implementation of the shooting method during the correcting process in the computation of the bifurcation branches through continuation methods.

A. Stability regions in the L_s - R_s plane

In general, there may be various feeder segments and load buses before the PCC. Therefore, at the best, the source and feeder impedances are the Thevenin equivalent obtained by looking into the network at the PCC. Thus, not only is the feeder impedance unknown a priori, it may suddenly change depending on the loads connected upstream. A non-stiff source supplying a load is shown in Fig. 4. Here, υ_s, R_s, and L_s represent the Thevenin equivalent looking towards the left in the network. The nonlinear load is a three phase EAF [32] looking towards the right into the network. In addition, there is a filter capacitor connected at the PCC bus. Since the Thevenin equivalent can change any time depending on the load at the left side of PCC, it is desirable to assess the set of υ_s, R_s, and L_s, for which the DTATCOM performance is stable.

For the electric system shown in Fig. 4, only the Neimark-Sacker bifurcation [1]-[2] was located in the parametrical space used in this analysis. The generalized Hopf bifurcation or Neimark-Sacker bifurcation is found when two complex conjugated Floquet multipliers leave the unit cycle. This bifurcation corresponds to a quasiperiodic solution. The Fig. 8 shows the bifurcation set on the L_s - R_s plane for different Thevenin voltages. The solid line represents the Neimark-Sacker bifurcation set. Inside the contour line the solutions are T-periodic, and the dark zone is the unstable region with a quasiperiodic behaviour. The stability regions for $|V_m|$=350 Volts, $|V_m|$=400 Volts, and $|V_m|$=440 Volts, are shown in Fig. 8(a), Fig. 8(b), and Fig. 8(c), respectively. In Fig. 8(d) a comparison is presented between the different stability boundaries; the stability region decrease as the source voltage becomes smaller. Also, Fig. 8(a) to Fig. 8(c) can be seen as bifurcation diagrams in the Thevenin space. These stability regions in the Thevenin space can be adjusted through a least-squares exercise to an analytical expression, thus, allowing to have the complete information on the three-dimensional space stability of the Thevenin equivalent, without having to show a bifurcation diagram in the L_s - R_s plane for each Thevenin voltage υ_s.

Selected waveforms for R_s=1 Ω, L_s=2 mH, and $|V_m|$=440 Volts are shown in Fig. 9. The voltage across the dc capacitor υ_{dc}, the terminal voltage υ_{ta}, and the angle δ are presented in Fig. 9(a), Fig. 9(b), and Fig. 9(c), respectively. This behaviour is in agreement with the solution predicted in Fig. 8(c), since for this set of parameters the bifurcation diagram predicts a quasiperiodic solution due to the Neimark-Sacker bifurcations. Please notice that for this operating point the dc voltage control given by (4) maintains the dc voltage oscillating around its reference. However, the DSTATCOM is not able to efficiently regulate the terminal voltage υ_t.

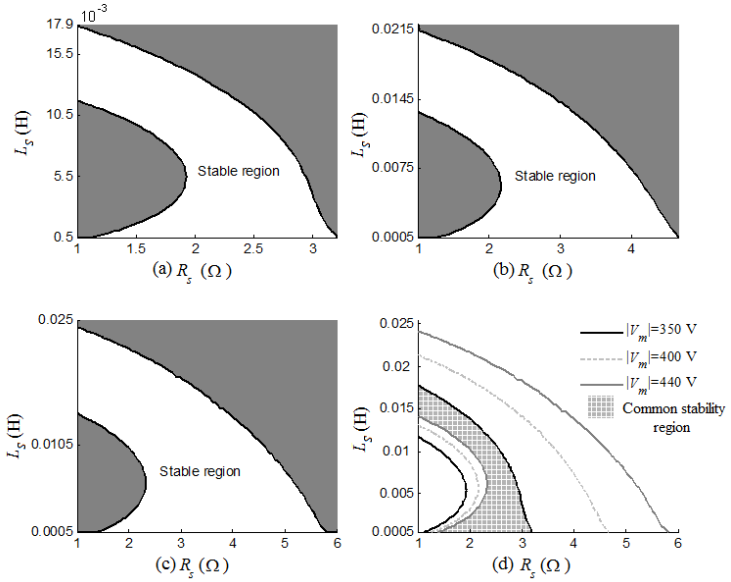

Fig. 8 Stability regions for the DSTATCOM operating in voltage control in the L_s - R_s plane for different Thevenin equivalent voltages; (a) $|V_m|$=350 Volts, (b) $|V_m|$=400 Volts, and (c) $|V_m|$=440 Volts. (d) Comparison of the stability boundaries.

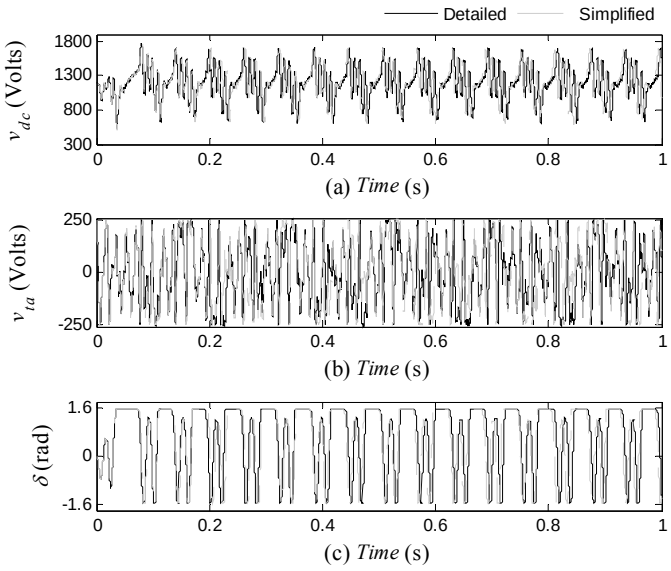

Fig. 9 Time domain solutions. (a) v_{dc}, (b) v_{ta}, and (c) i_{sa} for R_s=1 Ω, L_s=0.2 mH, and $|V_m|$=440 Volts.

Figure 8(d) shows that the only region for which the DSTATCOM properly operates in the Thevenin space for $|V_m|$ from $|V_m|$=350 Volts to $|V_m|$=440 Volts; is between the inner stability boundary of $|V_m|$=440 Volts and the outer stability boundary of $|V_m|$=350 Volts .In this region, the DSTATCOM can compensate any disturbance from the network. To corroborate this observation, various time domain simulations were carried-out for different Thevenin voltages. The R_s - L_s set used for these simulations were R_s=1 Ω, and L_s=20 mH. Initially, the system including the passive filter capacitor is in periodic steady-state with the nominal parameters given in the Appendix A; then, the DSTATCOM is connected at t=0 s. At t=0.5 s the Thevenin voltage magnitude is changed from $|V_m|$=440 Volts to $|V_m|$=400 Volts; for this operating point, the DSTATCOM properly compensates, as we expected from Fig. 8(d). However, when $|V_m|$ is decreased to $|V_m|$=380 Volts for $t \in [1, 1.7)$ s, the electric system becomes unstable and a quasiperiodic solution appears. At t=1.7 s $|V_m|$ is increased to $|V_m|$=500

Volts; for this operating point the DSTATCOM correctly compensates. Now, $|V_m|$ is increased to $|V_m|$=850 Volts at t=2.2 s; for this operating point a Neimark bifurcation appears. All these changes in the Thevenin voltage are shown in the waveforms of Fig. 10. The dc capacitor voltage υ_{dc} is shown in Fig. 10(a) and the angle δ in Fig. 10(b). Please notice that the detailed and the simplified models are used to conduct the time domain simulation; both models are in excellent agreement. These observations agree with the bifurcation diagrams shown in Fig. 8. To illustrate the quasiperiodic solution at $|V_m|$=850 Volts, the phase portrait in the υ_{dc} - δ plane is shown in Fig. 11. $|V_m|$=850 Volts is not a typical operating point, since for this voltage the protection system must open to disconnect the DSTATCOM from the PCC; however, it is useful to corroborate through time domain simulation the reliability of the bifurcation diagrams shown in Fig. 8.

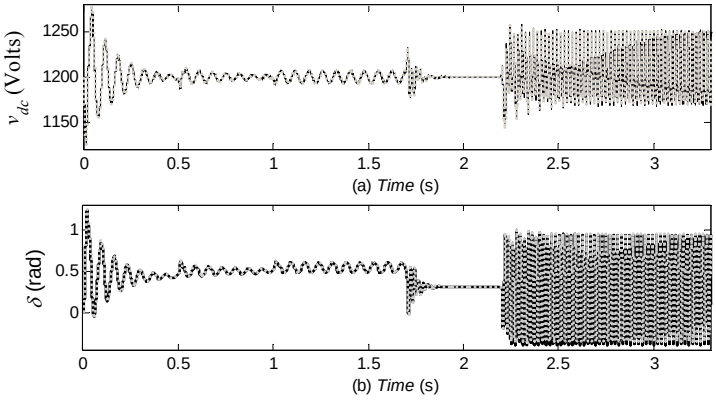

Fig. 10 Time domain solutions. (a) v_{dc}, (b) δ, and (c) v_{ta}

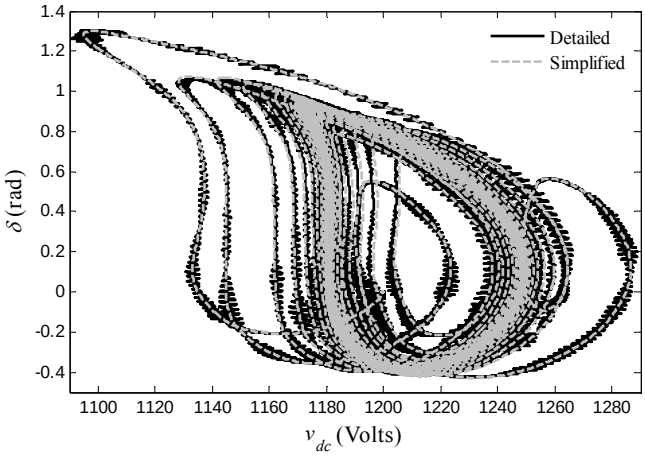

Fig. 11 Phase portrait in the v_{dc} - δ plan for $|V_m|$=850 Volts.

B. Stability regions in the gains plane.

The dynamic behaviour of the DSTATCOM in transient state is strongly related to the gain of the PI controllers; therefore, an important task is the proper gains assessment. In addition, the set of gains has an important impact on the DSTATCOM steady state performance, since they modify the stability regions.

In this section the stability region in the K_{idc} - K_{pdc} space, and in the $K_{i\delta}$ - $K_{p\delta}$ space are computed, as

well as the contour lines for different Floquet multipliers, with the purpose of assessing the set of gains for which the fastest speed of response is obtained.

Fig. 12(a) shows the stability in the $K_{i\delta}$ - $K_{p\delta}$ space, and Fig. 12(b) in the K_{idc} - K_{pdc} space. Also, in these figures, contour lines are presented for different Floquet multipliers to show the different speed of response. Figure 13(a) shows the convergence error for different pairs of gains $K_{i\delta}$ - $K_{p\delta}$. In Fig. 13(a), the convergence error for $K_{p\delta}$=30×10^{-6}, and different $K_{i\delta}$ are shown. From this figure, we can see that the fastest response is around $K_{i\delta}$=10.5×10^{-3} and $K_{p\delta}$=30×10^{-6}. Figure 13(b) shows the convergence error for K_{pdc}=74, and different K_{idc}. From this figure, it is easy to see that the fastest response is around K_{pdc}=74 and K_{idc}=1320. These results are in agreement with the bifurcation analysis illustrated in Fig. 12(a) and Fig. 12(b), respectively.

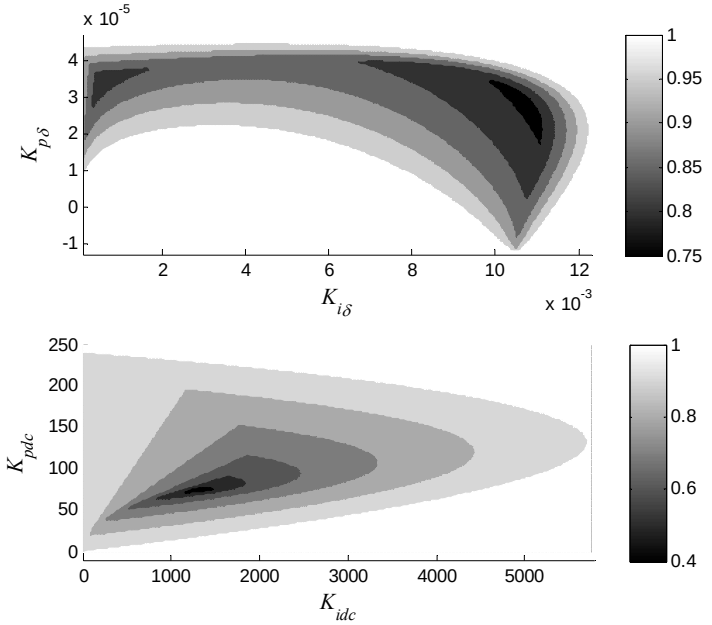

Fig. 12 Stability regions for the DSTATCOM operating in voltage control mode. (a) K_{idc} - K_{pdc} space. (b) $K_{i\delta}$ - $K_{p\delta}$ space.

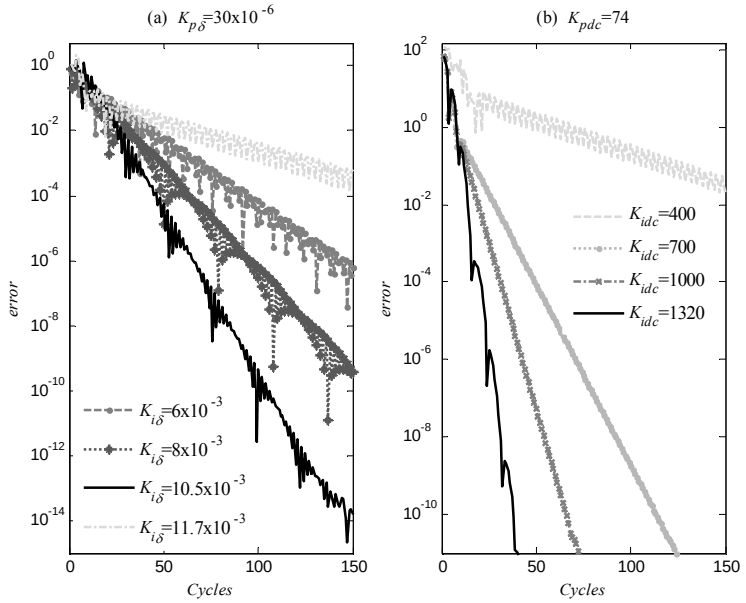

Fig 13 Convergence error for different gains of the DSTATCOM controllers. (a) For δ controller. (b) For the dc capacitor voltage controller.

As mentioned previously, the gains of the PI controllers have a direct impact on the stability system. However, it is not known how the size of the stable region in the Thevenin space varies when the gains are varied. To investigate the effect of the gains variation in the stability of the system, a bifurcation analysis is carried-out to assess the stable and unstable regions for different set of gains. In particular, the stability region obtained for K_{idc}=1320, K_{pdc}=74, $K_{i\delta}$=8×10^{-3}, and $K_{p\delta}$=27×10^{-6} with $|V_m|$=440 Volts is compared with that shown in Fig. 8(c). This comparison is shown in Fig. 14; it can be noticed that the size of the stable regions significantly change as we change the set of gains. Figure 14 has been computed using the parameters given in Appendix A; only the gains are varied.

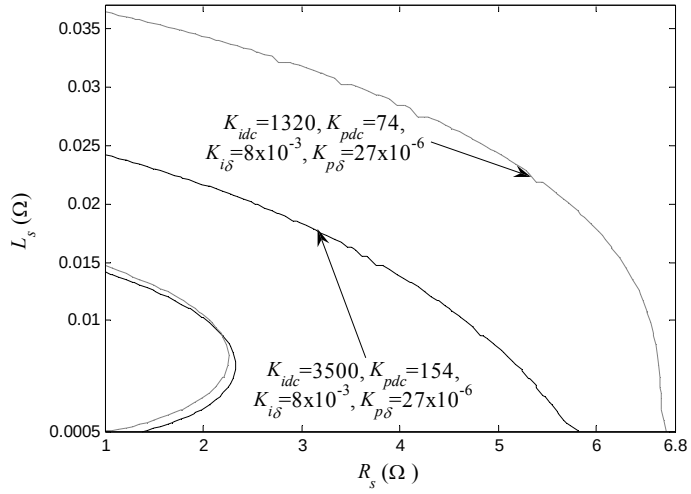

Fig. 14 Comparison between the stability regions for two sets of gains.

The bifurcation diagrams only show the stability over a parametric region, these do not give us information about the set of initial conditions for which the trajectories go back to their original steady-state. With the purpose of showing which set of gains shown in Fig. 14 has a larger attractor, a voltage sag of 41% is produced, and it is defined through simulation that the stability critical recovery time for the set of nominal gains presented in Appendix A, named set I, is t_a=0.0212 s. For the set of gains K_{idc}=1320, K_{pdc}=74, $K_{i\delta}$=8×10^{-3}, and $K_{p\delta}$=27×10^{-6}, named set II, t_b=0.175 s; the relationship t_b / t_a is 8.25 between the two different sets of gains. For the case of set I, the maximum Floquet multiplier for $|V_m|$=440 Volts and $|V_m|$=260 Volts is 0.88 and 1.43, respectively. For the set II, the maximum Floquet multiplier for $|V_m|$=440 Volts and $|V_m|$=260 Volts is 0.45 and 1.07, respectively. The maximum Floquet multiplier gives information about the limit cycle stability. As previously described, values within the unit circle indicate stable solutions, while external values to the unit circle correspond to unstable solutions. However, it also gives information about the speed of damping attenuation or increase of possible perturbations around the limit cycle. For instance, values close to the unit circle have slow dynamics, whereas farther away values have faster dynamics.

For the case of the response obtained for the set I, it is noticed that the Floquet multiplier in $|V_m|$=260 Volts is larger than the corresponding for set II. Therefore, the trajectories during the voltage sag go away more rapidly from the limit cycle corresponding to $|V_m|$=440 Volts for the set I. Thus, in a lesser time the state vector for the set I is outside of the attractor region for the limit cycle corresponding to $|V_m|$=440 Volts.

In conclusion, the set II is better than the set I for three main reasons: First, the response in nominal operation condition is faster, as shown in Fig. 12. Second, the size of the stable region in the L_s - R_s plane is bigger than the corresponding region for the set I, as shown by Fig. 14, and third, its dynamics

during the voltage sag are slower, and therefore, it withstands longer duration disturbances.

Figures 15(a) and 15(b), show the waveforms for δ and the voltage v_{dc} across the dc capacitor, respectively, for the set I of gains. In these figures, the steady state is shown for the first 150 ms; in t=150 ms the source voltage drops 41% and it is maintained over 21.2 ms; it then recovers to its pre-fault steady-state, with the DSTATCOM successfully compensating the system. Figs. 15(c) and 15(d) show the waveforms for δ and the voltage v_{dc} across the capacitor for the set II of gains, respectively. The waveforms are obtained as determined for set I, being the only difference the voltage sag lasting 175 ms.

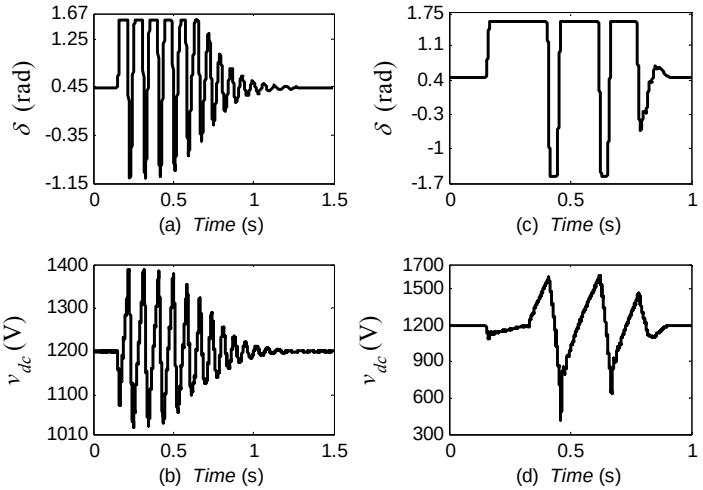

Fig. 15 Comparison between the transient responses for two sets of gains.

C. dc capacitor impact on the stability region

The dc capacitor is a very important element for the DSTATCOM design, as it stores the necessary energy to compensate the load during disturbances. In steady state, the DSTATCOM has to provide the active power fluctuation and the reactive power demanded by the system, in order to maintain the voltage at the PCC bus. Thus, the dc capacitor size is important for the compensator performance; e.g. for large capacitances, the storage energy is high; consequently, the DSTATCOM can bear larger and more severe disturbances. This observation suggests that the stable region increases as the dc capacitor size becomes larger. To corroborate this, a comparison between the stability regions for different dc capacitor sizes is presented in Fig. 16. It can be seen that the stable regions on the L_s - R_s asymptotically increases as the dc capacitor becomes larger. Please notice that even the inner unstable region decreases as the ac capacitor size increases. Figure 16 has been computed using the parameters given in Appendix A. From this analysis, the dc capacitor size can be selected to suit the load demand. Obviously, the selected dc capacitor size also depends on its cost.

D. ac capacitor filter impact on the stability region

The main purpose of the ac capacitor filter is to drain the harmonic currents coming from the DSTATCOM converters. A small ac capacitor size presents a high impedance to the harmonic currents; in consequence, the harmonic currents are not efficiently drained. For a large ac capacitor size, the harmonic currents are efficiently drained; however, there are some problems with a large ac capacitor filter. For instance, the transients in a capacitor increase as its size increases. To assess the ac

capacitor filter impact on the stability, the stable regions in the Thevenin plane have been compared for three different ac capacitors; this comparison can be seen in Fig. 17. From this figure, it easy to notice that the ac capacitor has a positive impact on the stability, since the stable region on the L_s - R_s plane increases as the ac capacitor becomes larger. However, it should be noticed that not only the outer boundary increases; the inner boundary becomes larger as well. Basically, the ac capacitor filter size has a positive effect on the stability because the ac capacitor acts also as a reactive power compensator, and this action reduces the reactive power injected by the DSTATCOM to maintain the reference terminal voltage. Figure 17 has been computed using the parameters given in Appendix A.

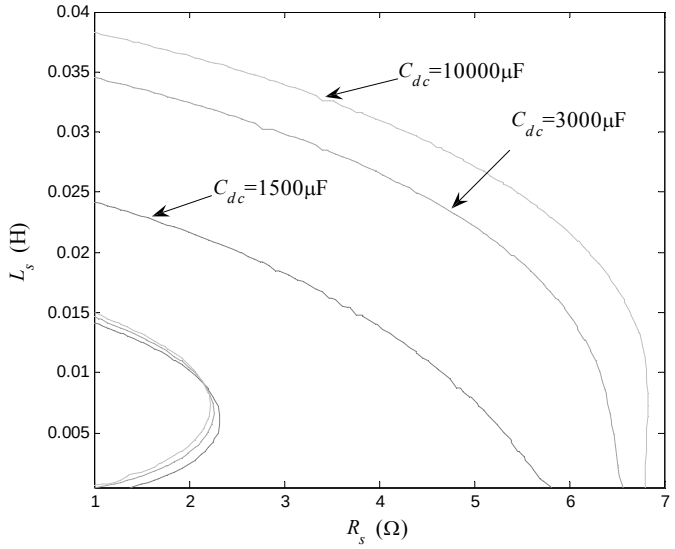

Fig. 16 Comparison between the stability regions for different dc capacitors.

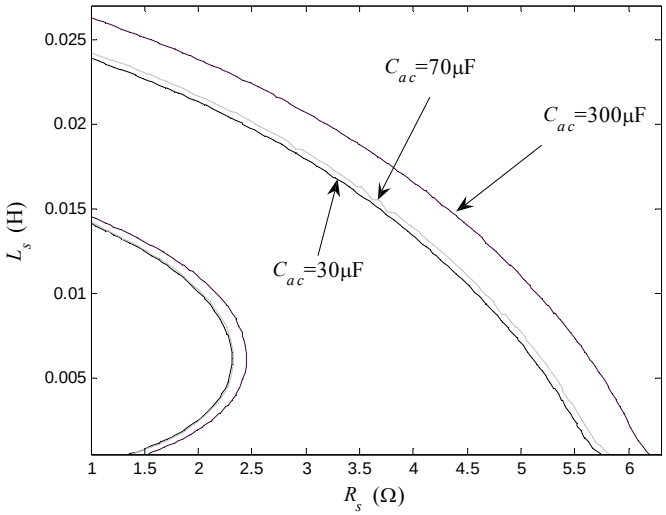

Fig. 17 Comparison between the stability regions for different ac capacitors.

V. CONCLUSION

The bifurcation theory has been applied to compute the nonlinear oscillations of the DSTATCOM

operating in voltage control mode; it allowed delimiting the stable region for which the DSTATCOM is able to keep constant the voltage at the PCC bus. This analysis has been conducted using the proposed simplified DSTATCOM model based on a state space approach.

It has been demonstrated that by adjusting certain system parameters, the system exhibits loss of stability due to the emergence of a Neimark bifurcation.

Bifurcation diagrams in the Thevenin space has been computed to show the impact on the stability due to voltage variations, as well as Thevenin impedance variations. The variations in the voltage source are associated to voltage sags and voltage swells, as well as disturbances in the network. The connection and disconnection of loads change the Thevenin impedance; it was previously mentioned that the source side impedance is, at the best, the Thevenin impedance looking towards the source from the bus controlled by the DSTATCOM.

In addition, the bifurcation diagrams in the gains space have been presented. From this analysis, the set of gains for which the DSTATCOM operates in a stable region can be obtained. The assessed set of gains for the fastest response of the DSTATCOM has been obtained.

The ac capacitor and dc capacitor impact on the stability has been assessed through bifurcation analysis. It has been demonstrated that both, ac and dc capacitor increase, have a positive impact on the stability.

A stability analysis has been carried-out for a particular compensation algorithm and for a particular nonlinear load; however, this analysis can be extended to any other algorithm for nonlinear load compensation to assess the stability boundaries for each case.

ACKNOWLEDMENT

The authors acknowledge the facilities granted by the DEP-FIE, of UMSNH and the Faculty of Built Environment and Engineering, of QUT to carry out this investigation. Juan Segundo acknowledges the scholarship granted by CONACYT to support his Doctoral studies at the DEP-FIE of the UMSNH.

REFERENCES

[1] T. S. Parker and L. O. Chua, “Practical Numerical Algorithms for Chaotic Systems”, Springer-Verlag, New York, 1989.

[2] A. H. Nayfeh and B. Balachandran, Applied nonlinear dynamics: analytical, computational, and experimental methods. New York: John Wiley & Sons, 1995.

[3] M. K. Mishra, A. Ghosh, and A. Joshi, “Operation of a DSTATCOM in voltage control mode,” IEEE Trans. Power Del., vol. 18, no. 1, pp. 258-264, Jan. 2003.

[4] P. Kundur, Power System Stability and Control, New York: McGraw-Hill, Inc., 1994.

[5] I. Dobson and H. D. Chiang, “Toward a theory of voltage collapse in electric power systems,” Syst. Contr. Lett., vol. 13, pp. 253–262, 1989.

[6] A. Medina, M. Gómez, and C.R. Fuerte, “Application of Bifurcations Theory to Assess Nonlinear Oscillations Produced by AC Electric Arc Furnaces,” IEEE Trans. Power Del.., vol. 20, pp. 801–806, Apr. 2005.

[7] H. O. Wang, E. H. Abed, and A. M. A. Hamdan, “Bifurcation, chaos and crisis in voltage collapse of a model power system,” IEEE Trans. Circuits Syst., vol. 41, no. 3, pp. 294–302, Mar. 1994.

[8] F. Wörnle, D. Harrison, and C. Zhou, “Analysis of a Ferroresonant Circuit Using BifurcationTheory and Continuation Techniques,” IEEE Trans. Power Delivery, vol. 20, pp. 191–196, Jan. 2005.

[9] S. H. Lee, J. K. Park, and B. H. Lee, “A study on the nonlinear controller to prevent unstable Hopf bifurcation,” in IEEE Power Eng. Soc. Summer Meeting, vol. 2, Jul. 2001, pp. 978–982.

[10] W. D. Rosehart and C. A. Cañizares, “Bifurcation analysis of various power system models,” Int. J. Elect. Power Energy Syst., vol. 21, no. 3, pp. 171–182, Mar. 1999.

[11] C. A. Cañizares, “On bifurcations, voltage collapse and load modeling,” IEEE Trans. Power Syst., vol. 10, pp. 512–522, Feb. 1995.

[12] M. A. Pai, P.W. Sauer, and B. C. Lesieutre, "Structural stability in power systems effect of load models," IEEE Tran. Power Syst., vol. 10, pp. 609–615, Feb. 1995.
[13] T. K. Vu and C. C. Liu, "Analysis of tap-changer dynamics and construction of voltage stability regions," IEEE Trans. Circuits Syst., vol. 36, no. 4, pp. 575–590, Apr. 1989.
[14] K. N. Srivastava and S. C. Srivastava, "Elimination of dynamic bifurcation in power systems using FACTS," IEEE Trans. Circuits Syst., vol. 45, no. 1, pp. 72-78, Jan. 1998.
[15] N. Mithulananthan, C. Cañizares, J. Reeve, and G. J. Rogers, "Comparison on PSSS, SVC and STATCOM controllers for damping power systems oscillations," IEEE Trans. Power Syst., vol. 18, no. 2, pp.786-792, May 2003.
[16] A. Azzouz, R. Duhr, and M. Hasler, "Transition to Chaos in a Simple Nonlinear Circuit Driven by Sinusoidal Voltage Source", IEEE Trans. Power Syst., vol. CAS-30, no. 12, Dec. 1983, pp. 913-914.
[17] Z. T. Zhusubaliyev, and E. Mosekilde, "Torus Birth Bifurcation in a DC/DC converter", IEEE Trans. on Circ. And Syst.-I, vol.53, no. 8, Aug. 2006, pp. 1839-1850.
[18] S. Jalali, I. Dobson, R. H. Lasseter, and G. Venkataramanan, "Switching Time Bifurcation in a Thyristor Controlled Reactor", IEEE Trans. on Circ. And Syst.-I, vol. 43, no. 3, March 1996, pp. 209-218.
[19] M. di Bernardo, and F. Vasca, "Discrete-Time Maps for the analysis of Bifurcations and Chaos in DC/DC Converters", IEEE Trans. on Circ. And Syst.-I, vol. 47, no. 2, Feb. 2000, pp. 130-143.
[20] M. di Bernardo, F. Garofalo, L. Glielmo, and F. Vasca, "Switching, Bifurcation, and Chaos in DC/DC Converters", IEEE Trans. on Circ. And Syst.-I, vol. 45, no. 2, March 1998, pp. 133-218-141
[21] Iu, H.H.C.; Robert, B. "Control of chaos in a PWM current-mode H-bridge inverter using time- delayed feedback" , IEEE Trans. on Circ. And Syst.-I, vol. 50, no. 8, March 2003, pp. 1125-218-1129.
[22] Chi Kong Tse, Complex behavior of switching power converters. New York:CRC Press, 2004.
[23] J. H. B. Deane, and D. C. Hamill, "Instability, Subarmonics, and Chaos in Power Electronic Systems", IEEE Trans. Power Del., vol. 5, no. 3, March 1990, pp. 260-268.
[24] G. Ledwich and A. Ghosh, "A flexible DSTATCOM operating in voltage or current control mode," *IEE Proc.-Gener. Transm. Distrib*., vol. 149, no. 2, pp.215-224, March 2002.
[25] H. Akagi, Y. Kanazawa, and A. Nabae, "Instantaneous reactive power compensators comprising switching devices without energy storage components," IEEE Trans. Ind. Applicat., vol. IA-20, pp. 625–630, May/June 1984.
[26] H. Akagi, A. Nabae, and S. Atoh, "Control strategy of active power filters using multiple voltage-source PWM converters," IEEE Trans. Ind. Applicat., vol. IA-22, no. 3, pp. 460–465, May/June 1986.
[27] A. Ghosh and A. Joshi , "A new approach to load balancing and power factor correction in power distribution system," IEEE Trans. Power Delivery, vol. 15, pp. 417–422, Jan. 2000.
[28] M.K. Mishra, A. Ghosh, and A. Joshi, "Load compensation for systems with non-stiff source using state feedback", Electric Power Systems Research, vol. 67, pp. 35-44, 2003.
[29] A. Ghosh and G. Ledwich, "Load compensating DSTATCOM in weak ac systems", IEEE Trans. Power Delivery, vol. 18, no. 4, pp.1302-1309, Oct. 2003
[30] TEQSIM International Inc., "Power System Blockset User´s Guide," 2001.
[31] A. Semlyen and A. Medina, "Computation of Periodic Steady-state in System With Nonlinear Components Using a Hybrid time and Frequency Domain Methodology", IEEE Trans. Power Syst., vol. 10, no. 3, pp. 1498-1504, August 1995.
[32] Acha E., Semlyen A., y Rajakovic N. "A Harmonic Domain Computation Package for Nonlinear Problems and its Application to Electric Arcs", IEEE Transactions on Power Delivery, vol 5, no. 3 July 1990, pp. 1390-1397.

APPENDIX A

The electric circuit parameters, the electric parameters of the DSTATCOM, and the control parameters are given in Table I.

TABLE I
SYSTEM PARAMETERS

Systems Parameters	DSTATCOM Voltage Mode
System voltage (V_s): 440 V (peak), sinusoidal and may contain harmonics,	Voltage controllers gains of dc capacitor loops: K_{pdc}=154, K_{idc}=3500.

exhibit sags and swells, and possible unbalance.	
Feeder impedance (R_s, L_s): 1+j 7.54 Ω	δ control loop gains: $K_{p\delta}$ =27e-6, $K_{i\delta}$=8e-3.
ac capacitor (C_{ac}):70 μF	dc capacitor(C_{dc}): 1500 μF
Feeder load impedance (R_l, L_l): 0.5+j 3.77 Ω	Interface circuits (R_f, L_f): 0.05+ j 3.77 Ω
EAF constants: K_1=15, K_2=0.05, K_3=800, m=0 and n=2.	Reference value of dc capacitor voltage: 1200 V